HIGH TEMPERATURE BEHAVIOUR OF A SINTERED β'-SIALON MATERIAL

G.Orange+, J.C.Glandus*, G.Fantozzi+, P.Boch*

The β'-Sialon material is a ceramic alloying phase which has the same combination of desirable properties than Si_3N_4, and moreover can be easily sintered to full density. The temperature dependence of elastic modulus, flexural strength and toughness has been examined up to 1500°C, in air and inert atmosphere. The high temperature mechanical behaviour is discussed in terms of microstructure.

INTRODUCTION

The high temperature properties of silicon nitride make it an ideal material for ceramic gas turbine components and other high performance applications. However, this material cannot be easily densified and so requires activated sintering processes such as hot pressing with densification additives or rection sintering. In order to promote the sintering ability of silicon nitride, new compounds derived from silicon nitide and oxynitride by simultaneous replacement of silicon and nitrogen by aluminium and oxygen were developed. The resulting sialon has the same combination of desirable properties than silicon nitride and can be densified by hot pressing or pressureless sintering as it has been shown by Jack(1).

The mechanical properties of ceramic materials are dominated by intrinsic microstructural variables which depend of elaboration processes. The experiments described in this paper were designed to determine the mechanisms of fracture in a pressureless sintered β'-sialon material, at room temperature and up to 1500°C. The microstucture dependence is well established and ways to improve this material can be deduced.

+ Groupe d'Etude de Metallurgie Physique et de Physique des Materiaux (LA 341), Bat 502 INSA, 69621 VILLEURBANNE, FRANCE.
* Laboratoire des Materiaux Ceramiques (LA 320), ENSCI, 87065 LIMOGES, FRANCE.

EXPERIMENTAL

Material

In the Si-Al-O-N system, the pure phases show extensive range of homogeneity along lines of constant metal to non-metal (M:X) ratio, but are extremely limited in other directions (fig.1). The β' phase, with the structure of β-Si_3N_4 and a range of homogeneity extending along the 3M:4X line, can be described by the formula $Si_{6-z}Al_zO_zN_{8-z}$ ($0 \leq z \leq 4.2$) as proposed by Lumby et al.(2). If the excess of SiO_2 in the Si_3N_4-Al_2O_3 mixture is not balanced, there is formation at 1700°C of the β' phase and a liquid phase which lead, on cooling , to the X phase (for high substitution level) or to the O' phase (low substitution level). Lewis et al. (3) have shown that these secondary phases can be reduced by increasing AlN content. However, the sintering ability is also reduced and additives must be used (MgO, Y_2O_3) to promote the densification.

The material* studied in this paper is obtained by pressure-less sintering , at 1700°C , with Y_2O_3 as additive. This material has a very low porosity (density d= 3.10 $g.cm^{-3}$) which is made of very fine independent pores. The prismatic grains are about 10 to 15 μm long. Unlike in the hot-pressed material, we don't observed any texture. The main constituant is β' phase, with a little amount of 15 R phase; the substitution level of this sialon is about z = 2.

Mechanical tests

The modulus of rupture and the elastic modulus have been measured up to 1500°C , in air and in controlled atmosphere (95% N_2 + 5% H_2) by three-points bending test (Orange et al.(4)). The specimens (25×5×3 mm^3) were loaded by means of alumina rollers (span : l= 21 mm). Values of Young's modulus were deduced from the applied load and actual deformation of specimens.

The critical stress intensity measurements (K_{Ic}) were achieved on single edge notched beam specimens (25×5×2.5 mm^3), with straigth-through and chevron notches (fig.2). For straight through notched specimens , K_{Ic} values were calculated according to the Brown and Srawley relation (5) , with a relative notch depth a/w of 0.4 and a notch tip radius of about 80 μm. The K_{Ic} values for the chevron notched specimens were obtained from the Munz et al. relation (6) , with $0.10 \leq \alpha_0 \leq 0.20$ and $\alpha_1 = 1$. The triangular notches were machined with a 100 μm width diamond saw. The advantage of chevron notched specimens is that a sharp crack is produced during loading and so K_{Ic} canbe evaluated from the initial specimens dimensions and the maximum load without requiring any crack length measurements as it has been shown by Barker (7) and Munz et al. (8). This method is quite interesting for ceramic materials which exhibit at high temperature important sub-critical crack growth.

All the tests were performed with a cross-head speed of 5.10^{-2} $mm.min^{-1}$.

*Sialon CERAVER (Usine de Bazet - 65001 TARBES , FRANCE) .

RESULTS

Elastic modulus and flexural strength

The elastic modulus , E , and flexural strength , σ_f , temperature dependence is shown in figures 3 and 4 respectively. There is no influence of short term oxydation. The three-points bending load-displacement curves indicate a plastic deformation only above 1300°C.

Critical stress intensity factor

The variation of K_Ic up to 1500°C , in air and nitrogen , is shown on figure 5. Above 1300°C , the β' sialon material exhibits a significant sub-critical crack growth and so it is necessary to take into account the variation of crack length during loading (a ⟶ a + da) with the straight-through notched specimens. Any plasticity effect has to be corrected so that value of K_Ic may be deduced from corrected crack length a + da. No correction is necessary with chevron notched specimens; moreover it is possible to integrate plasticity effect (if not important) during crack growth , with successive loading - unloading operations , and correct values of K_Ic may be obtained (Barker (9)).

Thermal shock behaviour

Thermal shock tests were made on rectangular section beams by quenching into room tempereture water according to the classical method (Glandus (10)). The critical temperature difference, ΔT_c , is measured as the temperature of quench which gives a decrease of the Young modulus (i.e. at the beginning of cracking). For the β'-sialon material studied here , the ΔT_c value is about 500°C.

DISCUSSION

Room temperature behaviour

This pressureless sintered β'-sialon material exhibits quite good mechanical properties. The flexural strength values , at room temperature , are just between the reaction-bonded and the hot-pressed silicon nitride one (11) . However , the fracture toughness is similar to that of best varieties of hot-pressed material. This is probably due to a specific microstructure made of elongated grains which increases the energy required to initiate and propagate cracks by a mechanism of pull-out of grains (12).

The fracture behaviour , at room temperature , is mainly controlled by not fully densified regions : these regions have a size equal to the critical defect (about 85 μm).

Lower values of fracture toughness have been reported for similar materials; this could be due to the presence of secondary phases (O' or X phase) , as it has been shown by Wills et al.(13) which affect the microstructure.

High temperature behaviour

Up to 1200°C, the mechanical behaviour is similar to that observed at room temperature : the fracture occurs by catastrophic propagation of cracks from critical defects.

Above 1200°C, the high temperature fracture behaviour is controlled by the grain boundary phases retained in the body during cooling from the sintering temperature. The grain boundary phase softens at high temperatures thus leading to slow crack growth and subsequent loss in strength. It is more the composition than the amount of grain boundary phase which is important and so the higher refractairity of the phase obtained by sintering with Y_2O_3 leads to less important subcritical crack growth than in sialon materials hot pressed with MgO (Karunaratne (14), Lewis et al (15)). Up to 1375°C, the grain boundary phase viscosity is high enough to increase the fracture surface energy and so the variation of K_{IC}. We can observe the formation of secondary cracks (fig. 6) which contribute also to the increase of K_{IC}. At higher temperature, the grain boundary phase viscosity is not sufficient enough and all the material characteristics fall off ; the fracture faces show a decohesion of grains (fig. 7).

It has been shown that thermal treatments (15) or oxidation (Lewis and Barnard (16)) could improve the mechanical behaviour of sialon. These developments, is combination with an optimisation of composition and elaboration processes, can lead to high performance material for engineering applications.

ACKNOWLEDGMENT

This work was supported by the French Research and Technology Department (under contract DGRST MAT/P 190 n° 79-7-0 865. The authors would like to express their gratitude to Mr. MINJOLLE of CERAVER COMPANY for supplying Sialon specimens.

REFERENCES

1. Jack K.H., 1976, J. Mat. Sci., 11, 1135

2. Lumby R.J., North B., and Taylor A.J., 1975, Special Ceramics 6, 283

3. Lewis M.H., Powell B.D., Drew P., Lumby R.J., North B, and Taylor A.J., 1977, J. Mat. Sci. 12, 61

4. Orange G., Dubois J., Fantozzi G., and Gobin P.F., 1980, Mem. Sci. Rev. Met., 2, 131

5. Brown W.F., and Srawley J.E., 1966, ASTM, S.T.P. n° 410

6. Munz D., Shannon J.L., and Bubsey R.T., 1980, Int. J.Fract. 16, 137

7. Barker L.M., 1977, Eng. Fract. Mech., 9, 361

8. Munz D., Bubsey R.T., and Srawley J.E., 1980, Int. J. Fract., 16, 359

9. Barker L.M., 1979, Int. J. Fract., 15, 515

10. Glandus J.C., Thesis, University of Limoges, 1981

11. Orange G., Epicier T., and Fantozzi G., 1980, Nitrogen Ceramics, to be published.

12. Evans A.G., Heuer A.H., and Porter D.L., 1977, Int. Conf. on Fracture 4, 1, 529

13. Wills R.R., Stewart R.W., and Wimmer J.M., 1977, Am. Ceram. Soc. Bull., 56, 194

14. Karunaratne B.S.B., and Lewis M.H., 1980, J. Mat. Sci., 15, 449

15. Lewis M.H., Bhatti A.R. Lumby R.J., and North B., 1980, J. Mat. Sci. 15, 103

16. Lewis M.H., and Barnard P., 1980, J. Mat. Sci., 15, 443

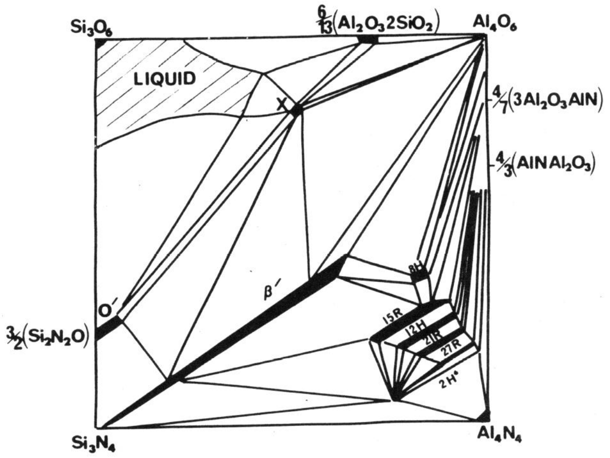

Figure 1 The Si_3N_4-AlN-Al_2O_3-SiO_2 system (1700°C)

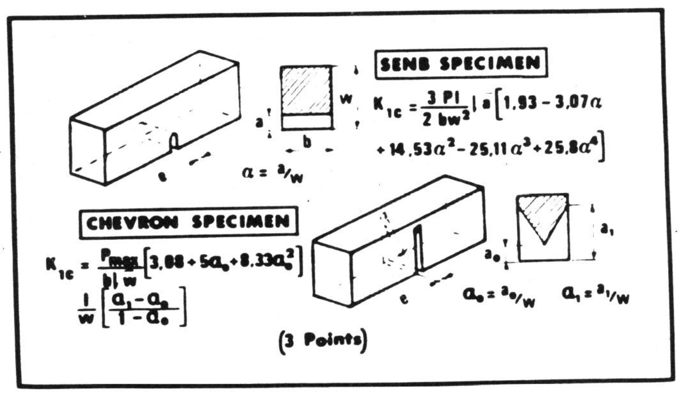

Figure 2 Fracture toughness specimens

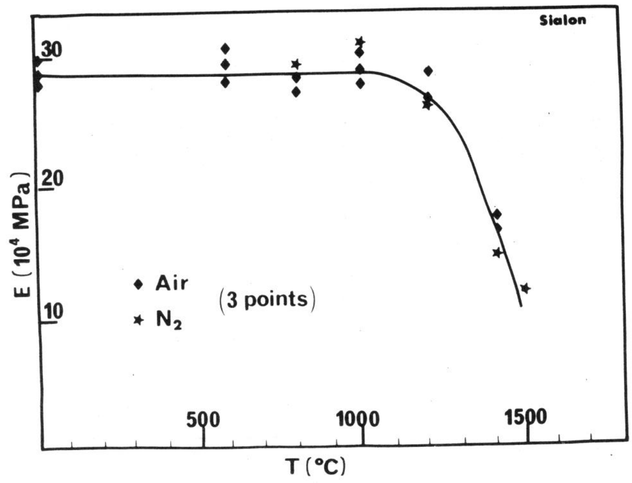

Figure 3 E(T) in air and N_2

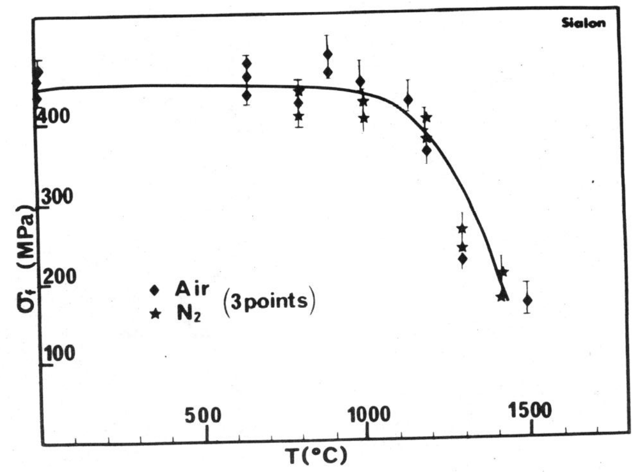

Figure 4 σ_f(T) in air and N_2

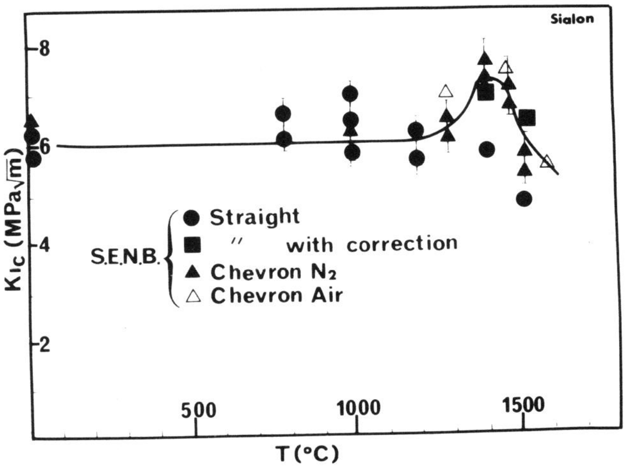

Figure 5 $K_{Ic}(T)$ with SENB specimens

a)

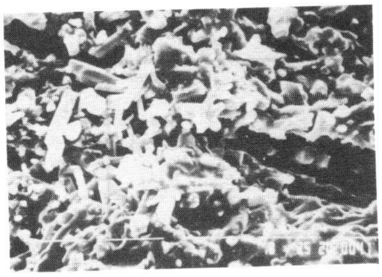

b)

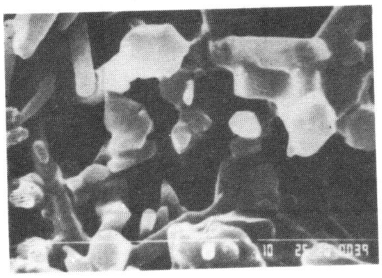

a)

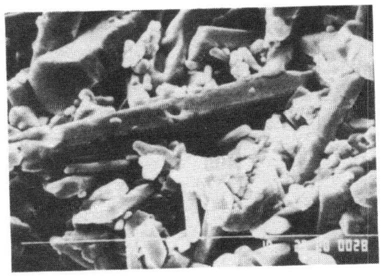

b)

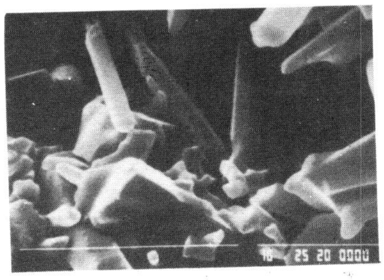

Figure 6 SENB fracture face (SEM)
a) 1300°C (N_2) b) Detail of a)

Figure 7 Flexural fracture face (SEM)
a) 1400°C (N_2) b) 1450°C (N_2)